Data supplement for Shanmugan et al., Common and Dissociable Mechanisms of Executive System Dysfunction Across Psychiatric Disorders in Youth. Am J Psychiatry (doi: 10.1176/appi.ajp.2015.15060725)

SUPPLEMENTARY METHODS

Participants: Exclusion Criteria

The Philadelphia Neurodevelopmental Cohort is a collaboration between the Center for Applied Genomics at CHOP and the Brain Behavior Laboratory at the University of Pennsylvania (Penn). Children, adolescents, and young adults between the ages of 8 and 21 who presented to the Children's Hospital of Philadelphia (CHOP) or a CHOP-affiliated clinic for a pediatric visit and volunteered to participate in genomic studies of complex pediatric disorders were eligible for inclusion in the Philadelphia Neurodevelopmental Cohort (1-3). Participants and/or their parents signed an informed consent form approved by the Institutional Review Boards at CHOP and Penn. After stratification by age and sex, a subsample of 1,601 randomly selected participants underwent multi-modal neuroimaging. Of these participants, 1,462 completed the n-back task described below. Subject exclusion criteria included medical conditions that might impact brain function (n=151), incidentally encountered structural brain abnormalities (n=20), and inadequate task performance (>7 nonresponses on the 0-back condition; n=65). As part of image quality assurance, subjects were also excluded for excessive motion (mean relative displacement > 0.5 mm or maximum displacement > 6 mm; n=94) or poor image coverage (n=73). Many of the subjects excluded met multiple exclusion criteria. The final sample included in analyses was 1,129. This sample thus constitutes a super-set of subjects previously included in reports which focused on normative development (4) and psychosis-spectrum symptoms (5).

Clinical Assessment

Psychopathology was assessed using a structured screening instrument (GOASSESS) administered by trained assessors (1). Participants age 11-21 were interviewed individually; collateral information was obtained independently from a caregiver for children age 8-17. To allow rapid training and standardization across a large number of assessors, GOASSESS was designed to be highly structured, with screen-level symptom and episode information. The instrument is abbreviated and modified from the epidemiologic version of the NIMH Genetic Epidemiology Research Branch Kiddie-SADS (6). Assessors underwent a common training protocol developed and implemented by MEC that included didactic sessions, assigned readings, and supervised pair-wise practice. They were certified for independent assessments through a standardized procedure requiring observation by a certified clinical observer who rated the proficiency of the assessor on a 60-item checklist of interview procedures.

The psychopathology screen in GOASSESS assessed psychiatric and psychological treatment history, as well as lifetime occurrence of major domains of psychopathology including mood (major depressive episode, mania), anxiety (agoraphobia, generalized anxiety, panic, specific phobia, social phobia, separation

anxiety), behavioral (oppositional defiant, attention deficit/hyperactivity, conduct), eating disorders (anorexia, bulimia), and suicidal thinking and behavior. Substance use disorders were assessed with a different instrument for a subset of participants and are not evaluated here. Each section included a screen for relevant symptoms and additional DSM-IV criteria such as symptom frequency, duration, onset, and offset. Associated distress and impairment were each rated on 11-point scales ranging from 0 to 10. To establish screening diagnostic criteria for each domain of psychopathology, a computerized algorithm integrated information regarding symptom frequency and duration approximating each DSM-IV disorder or episode criteria, accompanied by significant distress or impairment rated >=5 on the 11-point scale.

Assessment of Psychosis Spectrum Symptoms

As described in detail in our prior articles focused on psychosis-spectrum symptoms (5,7,8), GOASSESS provided three measures of psychosis-spectrum symptoms. First, sub-threshold positive symptoms in the past year were assessed with the 12-item assessor administered PRIME Screen-Revised (PS-R)(9). Items were read aloud by the assessor and self-rated on a 7-point scale (0 = Definitely Disagree; 6 = Definitely Agree). Second, lifetime threshold hallucinations and delusions were evaluated with the K-SADS (6) psychosis questions and structured follow-up probes. Third, negative and disorganized symptoms were evaluated using six assessor rated items from the Scale of Prodromal Symptoms (SOPS) in the Structured Interview for Prodromal Syndromes (SIPS)(10), including: N2 Avolition; N3 Expression of Emotion; N4 Experience of Emotions and Self; N6 Occupational Functioning; D3 Trouble with Focus and Attention; and P5 Disorganized Communication. We identified subjects as psychosis-spectrum if they: 1) had an age-deviant PRIME total score >= 2SD above age matched peers or had >= one PRIME item rated 6 or >= three items rated 5 (Somewhat Agree); 2) endorsed definite or possible hallucinations or delusions on the K-SADS psychosis screen; or 3) had an age deviant total negative/disorganized SOPS score >=2SD above age-matched peers.

Factor Analysis Methods

Factor analysis methods and results have been previously presented (11) and will be detailed in a separate manuscript (Calkins et al., In Preparation). Briefly, factor analyses proceeded in several phases. First, we performed exploratory factor analyses in order to determine which items loaded on which factors, with the ultimate goal of estimating a confirmatory factor analysis model from which to calculate scores. Because there are multiple exploratory factor analyses extraction methods (and an even greater number of factor rotations), we decided to estimate several exploratory factor analyses for thoroughness. Methods provided convergent results, supporting a four-factor model.

Because all exploratory factor analyses indicated *correlated* traits of psychopathology, and because a goal of the item-wise confirmatory analysis was to generate *orthogonal* scores, we opted to use the only type of confirmatory model capable of accommodating such a combination, which is the bifactor model (12-14).

Bifactor modeling is a way to estimate the contribution of an item to an overall dimension (psychopathology in this case) after controlling for its specific factor, and vice versa. Bifactor models are similar to higher-order models, except in a bifactor model there are direct effects of the general factor on the individual items.

The confirmatory bifactor model was estimated using the Bayesian estimator in Mplus (15). The Bayesian estimator comes with the drawback of not producing conventional fit indices, but was chosen because the computation time of other estimators (e.g. wlsmv) was anticipated to be much longer. The model was later estimated using the other estimators (wlsmv and MLR), and the minimum correlation between scores calculated using the different methods was 0.93 (mean = 0.98). The fit indices provided by the wlsmv-estimated model suggest acceptable fit, with a Comparative Fit Index (CFI) of 0.91 and Root Mean-Square Error of Approximation (RMSEA) of 0.027 ± 0.0005.

Task Paradigm

Subjects completed a fractal version of the n-back task (16) during their fMRI scan. During the task, a fractal was presented for 500 ms followed by a 2500 ms interstimulus interval. This task was used to probe working memory and had 3 conditions: 0-, 1-, and 2-back. During the 0-back, subjects responded by pressing a button when the fractal presented matched a predefined fractal. During the 1-back, subjects responded when the fractal presented was the same as the one preceding it. During the 2-back, subjects responded when the fractal was identical to the one two before it. Each condition consisted of three 20-trial blocks, each preceded by a 9s instruction period, with a target to foil ratio of 1:3. The task included a total of 45 targets and 135 foils, as well as three 24 s blocks of rest during which a fixation crosshair was displayed.

Image Acquisition

Imaging data were acquired on 3T Siemens TIM Trio whole-body scanner using a 32-channel head coil. A magnetization-prepared rapid acquisition gradient echo T1-weighted (MPRAGE) image (TR, 1810 ms; TE, 3.51 ms; TI, 1100 ms; FOV, 180 × 240 mm; matrix, 192 × 256; 160 slices; slice thickness/gap, 1/0 mm; flip angle, 9°; effective voxel resolution, 0.9 × 0.9 × 1 mm) and B0 field map (TR, 1000 ms; TE1, 2.69 ms; TE2, 5.27 ms; 44 slices; slice thickness/gap, 4/0 mm; FOV, 240 mm; effective voxel resolution, 3.8 × 3.8 × 4 mm) were acquired to aid spatial normalization to standard space and application of distortion correction procedures, respectively. Functional images were then obtained using a whole-brain, single-shot, multislice, gradient-echo echoplanar sequence (231 volumes; TR, 3000; TE, 32 ms; flip angle, 90°; FOV, 192 × 192 mm; matrix 64 × 64; 46 slices; slice thickness/gap 3/0 mm; effective voxel resolution, 3.0 × 3.0 × 3.0 mm).

Image Processing

As previously described (4), fMRI data was pre-processed with FSL (17), including skull removal with BET (18), slice time correction, motion-correction with MCFLIRT (19), spatial smoothing (6 mm FWHM), and mean-based intensity normalization. Subject-level timeseries analyses were carried out using FILM

(FMRIB's Improved Linear Model) with local autocorrelation correction (20). The three condition blocks (0-back, 1-back, and 2-back) were modeled using a canonical (double-gamma) hemodynamic response function with six motion parameters and the instruction period included as nuisance covariates. The rest condition served as the unmodeled baseline. The median functional and anatomical volumes were co-registered using boundary-based registration (21) with integrated distortion correction using FUGUE. The anatomical image was normalized to the Montreal Neurologic Institute 152 1 mm template using the top-performing diffeomorphic SyN registration of ANTS (22,23). All transformations (distortion correction, co-registration, normalization, and down-sampling to $2mm^3$) were concatenated so only one interpolation was performed. The statistical maps for the contrast of interest (2-back > 0-back) were then used in the group-level analyses. Statistical maps were downsampled further to $4mm^3$ for the multivariate distance-based matrix regression analysis (see below) for computational feasibility; generalized linear model analyses used $2mm^3$ resolution data.

Matrix Regression

Multivariate distance-based matrix regression operates in two steps. In the first step, the overall multivariate pattern of activation and de-activation in down-sampled data (4mm isotropic voxels) was compared among subjects using a distance metric (Euclidean distance). This produces a matrix (size 1,129 x 1,129) representing how similar the overall pattern of activation is between each combination of subject pairs. Second, matrix regression is used to test how well each phenotypic variable explains the distances between each participant's pattern of activation created in step 1. This provides a measure of how the overall pattern of activation is impacted by each group level variable entered into the design matrix in standard regression format. Our group-level design matrix included symptom dimensions (from the factor analysis), age, sex, and in-scanner motion. As in our prior work, motion was summarized for each subject as the mean relative displacement of realignment parameters across the time series (24-26). This multivariate distance-based matrix regression procedure yields a pseudo-F statistic, the significance of which was tested using 1,000 permutations.

SUPPLEMENTARY REFERENCES

1. Calkins ME, Merikangas KR, Moore TM, Burstein M, Behr MA, Satterthwaite TD, et al. The philadelphia neurodevelopmental cohort: Constructing a deep phenotyping collaborative. J Child Psychol Psychiatry 2015, Apr 8.
2. Satterthwaite TD, Connolly JJ, Ruparel K, Calkins ME, Jackson C, Elliott MA, et al. The philadelphia neurodevelopmental cohort: A publicly available resource for the study of normal and abnormal brain development in youth. Neuroimage 2015, Mar 31.
3. Satterthwaite TD, Elliott MA, Ruparel K, Loughead J, Prabhakaran K, Calkins ME, et al. Neuroimaging of the philadelphia neurodevelopmental cohort. Neuroimage 2014, Feb 1;86:544-53.

4. Satterthwaite TD, Wolf DH, Erus G, Ruparel K, Elliott MA, Gennatas ED, et al. Functional maturation of the executive system during adolescence. J Neurosci 2013, Oct 9;33(41):16249-61.
5. Wolf DH, Satterthwaite TD, Calkins ME, Ruparel K, Elliott MA, Hopson RD, et al. Functional neuroimaging abnormalities in youth with psychosis spectrum symptoms. JAMA Psychiatry 2015, Mar 18.
6. Kaufman J, Birmaher B, Brent D, Rao U, Flynn C, Moreci P, et al. Schedule for affective disorders and schizophrenia for school-age children-present and lifetime version (K-SADS-PL): Initial reliability and validity data. J Am Acad Child Adolesc Psychiatry 1997, Jul;36(7):980-8.
7. Gur RC, Calkins ME, Satterthwaite TD, Ruparel K, Bilker WB, Moore TM, et al. Neurocognitive growth charting in psychosis spectrum youths. JAMA Psychiatry 2014, Feb 5.
8. Calkins ME, Moore TM, Merikangas KR, Burstein M, Satterthwaite TD, Bilker WB, et al. The psychosis spectrum in a young U.S. Community sample: Findings from the philadelphia neurodevelopmental cohort. World Psychiatry 2014, Oct;13(3):296-305.
9. Kobayashi H, Nemoto T, Koshikawa H, Osono Y, Yamazawa R, Murakami M, et al. A self-reported instrument for prodromal symptoms of psychosis: Testing the clinical validity of the PRIME screen-revised (PS-R) in a japanese population. Schizophr Res 2008, Dec;106(2-3):356-62.
10. Miller TJ, Cicchetti D, Markovich PJ, McGlashan TH, Woods SW. The SIPS screen: A brief self-report screen to detect the schizophrenia prodrome. Schizophr Res 2004;70(Suppl 1):s78.
11. Moore TM. Latent dimensions underlying psychopathology and neurocognition: Discovery, modeling, and use in research; Presented at SOBP 2015.
12. Holzinger KJ, Swineford F. The bi-factor method. Psychometrika 1937;2(1):41-54.
13. Reise SP, Moore TM, Haviland MG. Bifactor models and rotations: Exploring the extent to which multidimensional data yield univocal scale scores. J Pers Assess 2010, Nov;92(6):544-59.
14. Reise SP. Invited paper: The rediscovery of bifactor measurement models. Multivariate Behav Res 2012, Sep 1;47(5):667-96.
15. Muthén B, Asparouhov T. Bayesian structural equation modeling: A more flexible representation of substantive theory. Psychol Methods 2012, Sep;17(3):313-35.
16. Ragland JD, Turetsky BI, Gur RC, Gunning-Dixon F, Turner T, Schroeder L, et al. Working memory for complex figures: An fmri comparison of letter and fractal n-back tasks. Neuropsychology 2002, Jul;16(3):370-9.
17. Jenkinson M, Beckmann CF, Behrens TEJ, Woolrich MW, Smith SM. FSL. Neuroimage 2012, Aug 15;62(2):782-90.
18. Smith SM. Fast robust automated brain extraction. Hum Brain Mapp 2002;17(3):143-55.
19. Jenkinson M, Bannister P, Brady M, Smith S. Improved optimization for the robust and accurate linear registration and motion correction of brain images. Neuroimage 2002;17(2):825-41.

20. Woolrich MW, Jbabdi S, Patenaude B, Chappell M, Makni S, Behrens T, et al. Bayesian analysis of neuroimaging data in FSL. Neuroimage 2009, Mar;45(1 Suppl):S173-86.
21. Greve DN, Fischl B. Accurate and robust brain image alignment using boundary-based registration. Neuroimage 2009, Oct 15;48(1):63-72.
22. Klein A, Andersson J, Ardekani BA, Ashburner J, Avants B, Chiang MC, et al. Evaluation of 14 nonlinear deformation algorithms applied to human brain MRI registration. Neuroimage 2009, Jul 1;46(3):786-802.
23. Avants BB, Tustison NJ, Song G, Cook PA, Klein A, Gee JC. A reproducible evaluation of ants similarity metric performance in brain image registration. Neuroimage 2011, Feb 1;54(3):2033-44.
24. Satterthwaite TD, Wolf DH, Loughead J, Ruparel K, Elliott MA, Hakonarson H, et al. Impact of in-scanner head motion on multiple measures of functional connectivity: Relevance for studies of neurodevelopment in youth. Neuroimage 2012, Jan 2;60(1):623-32.
25. Satterthwaite TD, Elliott MA, Gerraty RT, Ruparel K, Loughead J, Calkins ME, et al. An improved framework for confound regression and filtering for control of motion artifact in the preprocessing of resting-state functional connectivity data. Neuroimage 2013, Jan 1;64(0):240-56.
26. Satterthwaite TD, Wolf DH, Ruparel K, Erus G, Elliott MA, Eickhoff SB, et al. Heterogeneous impact of motion on fundamental patterns of developmental changes in functional connectivity during youth. Neuroimage 2013, Dec;83(0):45 - 57.

Figure S1.

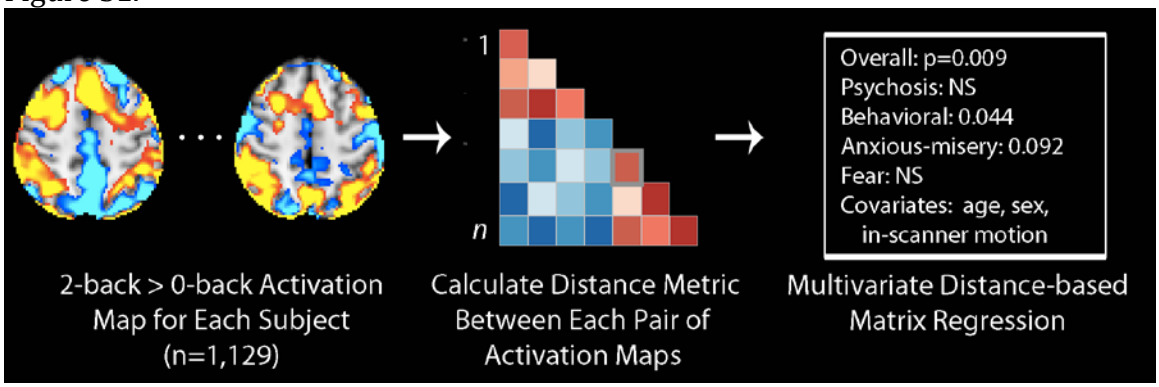
1
n
Overall: p=0.009
Psychosis: NS
Behavioral: 0.044
Anxious-misery: 0.092
Fear: NS
Covariates: age, sex, in-scanner motion
2-back > 0-back Activation Map for Each Subject (n=1,129)
Calculate Distance Metric Between Each Pair of Activation Maps
Multivariate Distance-based Matrix Regression

Table S1. Main effect of psychopathology dimensions in complete sample (n=1129)

Region	k	Peak *z*	x	y	z
HYPO-ACTIVATION					
Overall Psychopathology					
Frontal pole	993	4.96	-34	48	16
Precuneus cortex	752	4.54	10	-70	56
Frontal pole	698	5.07	30	44	20
Superior frontal gyrus	600	4.65	-2	10	56
Central operculum	283	4.9	-42	12	4
Precentral gyrus	172	4.26	-28	-8	60
Cerebellar crus I	167	4.56	34	-76	-22
Middle temporal gyrus	159	3.93	54	-44	4
Superior frontal gyrus	131	3.93	16	4	62
Anterior insula	131	3.94	22	30	4
Anterior cingulate gyrus	123	4.08	-8	14	28
Thalamus	104	3.92	-10	-20	16
Anterior cingulate gyrus	84	3.92	8	8	32
Psychosis					
Superior frontal gyrus	293	4.09	-22	-4	58
Fear					
Juxtapositional lobule cortex	118	3.91	-12	6	56
Behavioral					
Superior parietal lobule	641	4.49	38	-46	50
Supramarginal gyrus	568	4.88	-28	-46	38
Cerebellar crus I	510	3.88	-30	-52	-36
Cerebellar vermis crus II	477	3.92	0	-80	-28
Thalamus	440	4.45	6	-20	10
Middle frontal gyrus	319	4.58	-26	-4	56
Posterior cingulate gyrus	256	3.95	6	-28	26
Superior frontal gyrus	150	4.1	24	4	46
Juxtapositional lobule cortex	97	3.58	-6	8	58
Caudate	77	3.76	-8	4	2
Cerebellar V	77	3.99	-2	-58	-24
Anterior insula	69	3.85	-44	14	-8

Region	k	Peak *z*	x	y	z
HYPER-ACTIVATION					
Anxious Misery					
Superior frontal gyrus	863	5.12	0	10	68
Frontal pole	535	4.27	32	36	42
Paracingulate gyrus	454	4.51	8	12	42
Anterior insula	355	4.14	36	34	-2
Precentral gyrus	334	4.4	-32	-6	56
Angular gyrus	182	3.62	48	-46	18
Frontal pole	91	4.02	38	52	16
Angular gyrus	84	3.6	62	-60	24

Table S2. Differential effects of psychopathology dimensions in complete sample (n=1129)

Region	k	Peak *z*	x	y	z
Superior frontal gyrus	1459	5.51	18	-2	70
Frontal pole	575	4.72	32	44	20
Precentral gyrus	502	5.06	-32	-6	58
Middle temporal gyrus	355	4.16	54	-44	4
Frontal pole	320	4.4	-32	46	14
Inferior frontal gyrus	211	3.83	56	18	30
Superior temporal gyrus	115	4.68	-52	-8	-6
Anterior insula	95	3.89	34	32	-2
Precuneus	80	3.68	8	-72	52
Temporal occipital fusiform cortex	74	4.05	-38	-48	-20

Table S3. Main effect of psychopathology dimensions in sub-sample of participants not taking psychotropic medication (n=1007)

Region	k	Peak *z*	x	y	z
HYPO-ACTIVATION					
Overall Psychopathology					
Frontal pole	1686	5.43	-34	48	16
Superior frontal gyrus	1587	5.25	-2	10	56
Precuneus cortex	1455	4.71	10	-70	54
Frontal pole	823	5.09	34	44	26
Cerebellar crus VI	397	4.47	30	-60	-30
Middle temporal gyrus	249	4.11	54	-48	12
Lateral occipital cortex	150	3.85	-44	-58	58
Thalamus	126	4.05	-8	-20	16
Anterior insula	104	3.6	22	22	0
Middle frontal gyrus	86	3.89	-42	14	38
Occipital fusiform cortex	84	4.31	-42	-74	-24
Psychosis					
Superior frontal gyrus	97	3.62	-22	6	52
Superior parietal lobule	69	4.2	-30	-52	60
Superior parietal lobule	69	3.99	-18	-64	58
Fear	none				
Behavioral					
Superior parietal lobule	810	4.16	-38	-48	-18
Supramarginal gyrus	337	4.44	-28	-46	38
Superior parietal lobule	178	4.02	38	-46	50
Middle frontal gyrus	174	3.96	-26	-4	56
Precuneus cortex	128	3.75	14	-58	54
HYPER-ACTIVATION					
Anxious Misery					
Superior frontal gyrus	491	4.59	-2	12	68
Frontal pole	125	4.11	38	34	40
Paracingulate gyrus	124	3.91	6	12	44
Middle frontal gyrus	112	4.06	50	16	32

Table S4. Main effect of psychopathology dimensions with working memory performance (*d'*) as a covariate (n=1129)

Region	k	Peak *z*	x	y	z
HYPO-ACTIVATION					
Overall Psychopathology					
Frontal pole	330	4.41	28	44	20
Frontal pole	208	4.3	-30	48	26
Central operculum	139	4.29	-42	12	4
Psychosis					
Superior frontal gyrus	158	3.87	-24	6	52
Fear	none				
Behavioral					
Supramarginal gyrus	221	4.02	38	-46	52
Superior parietal lobule	124	4.18	-28	-46	38
Thalamus	69	3.63	6	-28	26
HYPER-ACTIVATION					
Anxious Misery					
Temporal pole	233	4.09	52	12	-22
Inferior frontal gyrus	232	3.97	52	30	-4
Middle frontal gyrus	219	4.13	36	0	46
Superior frontal gyrus	169	4.67	-2	12	70
Cingulate gyrus	152	4	8	12	40
Inferior frontal gyrus	131	3.93	56	16	32
Superior temporal gyrus	125	4.06	-52	-8	-6
Temporal pole	95	3.87	-44	8	-20
Supramarginal gyrus	78	3.52	62	-40	14

Table S5. Main effect of psychopathology dimensions while including additional covariates (n=1112 due to missing covariate data in 17 subjects). Covariates included: age, sex, race, in-scanner motion, maternal education, time between assessment and imaging, out-of-scanner cognitive performance, and in-scanner working memory performance.

Region	k	Peak *z*	x	y	z
HYPO-ACTIVATION					
Overall Psychopathology					
Frontal pole	448	4.57	30	42	18
Frontal pole	353	4.57	-32	48	16
Central operculum	153	4.32	-42	12	4
Middle temporal gyrus	102	3.92	54	-44	4
Precuneus cortex	87	3.71	10	-70	56
Psychosis					
Superior frontal gyrus	145	3.87	-22	-4	60
Fear	none				
Behavioral					
Supramarginal gyrus	73	3.98	-28	-46	38
HYPER-ACTIVATION					
Anxious Misery					
Anterior insula	224	3.98	50	32	-2
Middle frontal gyrus	198	4.02	36	0	46
Superior frontal gyrus	137	4.57	-2	12	70
Superior temporal gyrus	133	3.87	58	-4	-10
Inferior frontal gyrus	114	3.83	56	16	32
Middle temporal gyrus	110	3.61	62	-42	2
Frontal pole	107	3.86	8	12	40
Superior temporal gyrus	79	3.86	-52	-8	-6

Table S6. Main effect of psychopathology dimensions after excluding for poor 2-back performance (n=963)

Region	k	Peak *z*	x	y	z
HYPO-ACTIVATION					
Overall Psychopathology					
Frontal pole	376	4.38	28	44	20
Frontal pole	232	4.47	-34	48	16
Frontal operculum	226	4.68	-42	12	4
Precuneous cortex	206	4.46	10	-70	54
Supramarginal gyrus	138	4.28	56	-40	46
Thalamus	125	4.14	-4	-32	8
Superior frontal gyrus	120	4.1	-2	10	56
Fear	none				
Behavioral					
Thalamus	321	4.32	8	-20	6
Superior parietal lobule	244	4.45	-28	-46	38
Superior parietal lobule	215	4.11	38	-46	52
Cingulate gyrus	213	4.04	6	-30	26
Cerebellar VI	169	3.87	-18	-60	-22
Cerebellar Vermis VI	109	3.54	2	-72	-16
Caudate	97	3.93	-8	4	2
Superior frontal gyrus	83	4.01	-26	-2	58
HYPER-ACTIVATION					
Anxious Misery					
Cingulate gyrus	309	4	8	14	38
Middle frontal gyrus	152	3.99	36	0	46
Frontal pole	102	4.06	32	36	42
Superior frontal gyrus	75	4.38	0	10	68
Inferior frontal gyrus	73	3.65	56	16	32
Psychosis					
Cingulate gyrus	67	4.21	2	-44	14